ELSEVIER

Chemical Engineering Journal 70 (1998) 37–45

Chemical Engineering Journal

Scaling of turbulence characteristics in a turbine-agitated tank in relation to agitation rate

Eva Ståhl Wernersson *, Christian Trägårdh [1]

Food Engineering, Lund University, PO Box 124, S-221 00 Lund, Sweden

Received 16 December 1996; revised 23 December 1997; accepted 5 January 1998

Abstract

The influence of agitation rate on scaling in a turbine-agitated tank is examined using constant temperature anemometry measurements. Measurements in the high-intensity impeller zone are compared with measurements in the bulk zone for four agitation rates. The mean velocity of the flow was found not to be constant when scaled with V_{tip}. This is contrary to assumptions and measurements reported in the literature. The energy spectra in the impeller zone scale by the energy dissipation length scales and so did also the low wavenumbers of the spectra in the bulk zone. A small region of the energy spectra in the impeller zone are scaled by Kolmogorov's scales. In the bulk zone, the low-energy range of high wavenumbers of the energy spectra scale with Kolmogorov's scales. The ratios of energy dissipation rate and the ratios of turbulent kinetic energy in the impeller zone versus the bulk zone, show a linear increase as the agitation rate is increased. This indicates that changing the agitation rate affects flow conditions in the impeller zone more than in the bulk zone.

Keywords: Scale-up; Anemometry measurements; Agitated tank; Turbulence; Local energy dissipation rate; Agitation rate

1. Introduction

Scaling is important when designing bioreactors for full-scale production, but it is also important in the prediction of the performance of a certain process when parameters are changed in an existing reactor. Bioprocesses demand a high degree of energy input/unit mass and therefore mixing is dominated by turbulence. In a bioprocess, the microorganisms are of such a size that they are influenced by local turbulence conditions. It is thus important to study local turbulence conditions in turbine-agitated tanks.

The fluid dynamics in the reactor is closely linked to scale-up and mixing, since it is the flow that distributes heat and mass in the reactor. There are global parameters, which express average values for the whole process, but they do not take into consideration the local variations in flow or the turbulent quantities of the flow. The impeller Reynolds number is greater than 10^3 in turbine-agitated tanks for dispersion processes, while results in the literature show local Reynolds numbers ranging from 40 to 300 in the impeller zone (Mujumdar et al. [1]; Rao and Brodkey [2]; Günkel and Weber, [3]; Wu and Patterson [4]). The mean velocity, being important for the convective flow, which in turn determines the pumping capacity and the circulation capacity of the flow, is commonly considered to be constant, and to scale with the impeller tip speed, V_{tip}. In the literature a large tolerance to this scale-up criterion is found when profiles from several authors are compared (Kresta and Wood [5]) or when profiles from different agitation rates in the same equipment are compared (Cutter [6]).

The result of most turbulent flow measurements in turbine-agitated tanks are presented for different radial positions in the impeller zone. Only in a few articles is the agitation rate changed. Coustes and Couderc [7,8] concluded that turbulence characteristics could be normalized with n or d_{imp} or a combination of both. Cutter [6] and Wu and Patterson [4] have performed measurements at several agitation rates, but present their results of intensities and local energy dissipation rates for one agitation rate, after concluding that agitation rate did not influence their results to any great extent. Nishikawa et al. [9] compared energy spectra at different agitation rates and concluded that they could be scaled by the energy dissipation length, λ_f.

Abbreviations: CTA, Constant Temperature Anemometry; FFT, Fast Fourier Transform

* Corresponding author. Fax: +46-46-222-46-22; e-mail: eva.stahl_wernersson@livstek.lth.se

[1] E-mail: christian.tragardh@livstek.lth.se

1385-8947/98/$19.00
PII S1385-8947(98)00071-0

Results regarding turbulent kinetic energy are rather scarce in the literature, although this parameter is used to estimate the local energy dissipation rate using dimensional arguments. In earlier measurements, q was approximated to $\bar{u}_1^2$ since measurements were usually conducted in one direction only (Rao and Brodkey [2]; Cutter [6]; Coustes and Couderc, [7,8]; Laufhütte and Mersmann, [10]).

Kawase and Moo-Young [11], among others, identified the local energy dissipation rate per unit mass as being one of the most important parameters in the scale-up of dispersion processes. Their conclusion is based on theoretical application of Kolmogorov's theory which defines scales in time and length of the micro-eddies or the vortices of the flow.

The objective of this study was to investigate how the turbulent parameters, $\sqrt{\bar{u}_i^2}$, q and ε, as well as the energy spectra, scale with agitation rate, since this is a parameter related to the operating conditions in a process.

In this paper, turbulent velocity measurements in three directions of flow using constant temperature anemometry are described. A split-film probe was used in a pilot-scale turbine-agitated tank. Turbulence characteristics, i.e., turbulent intensity, turbulent kinetic energy, local energy dissipation rates and energy spectra were scaled with local parameters.

The flow was evaluated in flow coordinates, the reason being that the microorganisms in a fermentation process are affected by the magnitude and the intensity of this flow and not by the flow expressed in tank coordinates. In the literature regarding measurements on agitated tanks, the flow is usually expressed in tank coordinates.

2. Materials and methods

Experiments were conducted in a turbine-agitated tank with geometry, according to Fig. 1. The diameter of the tank, D_{tank}, was 0.8 m, the impeller size $D_{tank}/3$ and the tank was equipped with four baffles to prevent vortex formation. the tank was equipped with two Rushton turbines and the experiments were performed at the lower impeller in the position $2r/D_{tank} = 0.49$, at the centre line of the impeller and in the bulk zone: $2r/D_{tank} = 0.49$, $H_{v2} = 0.600$. The spacing between the impellers, ΔC, was $0.7D_{tank}$ and the off-bottom clearance was, C, was $0.425D_{tank}$. The total liquid height, H_L, was $1.50D_{tank}$. Degassed microfiltrated water was used as liquid and the temperature was kept constant, as required by the measuring method. The liquid surface was covered with a plastic lid to prevent surface aeration and the creation of bubbles in the liquid.

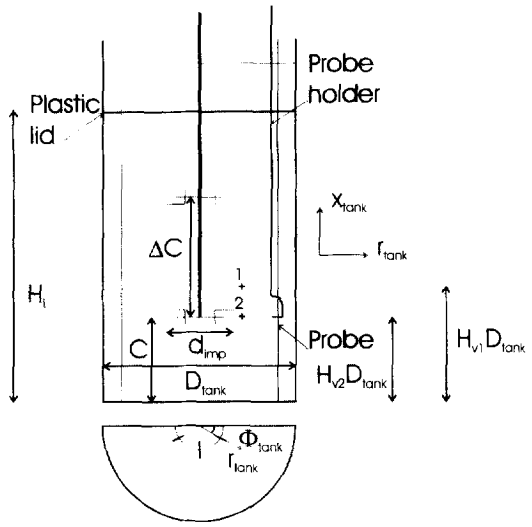

Fig. 1. View of the tank with probe holder, measuring locations and tank coordinates.

Turbulent velocities were measured with Constant Temperature Anemometry, CTA, using a two-channel system (DISA CTA 56C17) and a split-film probe especially designed for water (DANTEC R55). The probe has a measuring length of 1.25 mm and a diameter of 0.200 mm, and instantaneous velocities can be measured in two directions simultaneously.

The probe was inserted from the top of the reactor, 30° from the baffle (see Fig. 1). The probe holder was rotated until the split faced the convective direction of the flow, which was 45° from the radial tank direction on the plane of the turbine. The instantaneous velocities were referred to flow coordinates according to Figs. 2 and 3. Velocities were measured for all three directions of flow. Two different probe holders were used, one locating the probe in the radial/axial (r_{tank}, x_{tank}) plane of the tank, Fig. 2, and one locating the probe in the radial/tangential (r_{tank}, Φ_{tank}) plane of the tank, Fig. 3. Calibration was carried out before and after measurements, using a special calibration unit, to ensure the stability of the measuring system. Details on calibration are given elsewhere (Ståhl Wernersson and Trägårdh [12]).

Voltages from the two-channel system were connected to an A/D converter with a sample-and-hold card, CIO-AD16JR-AT (Computer Boards). The data were analysed using several programs written in Fortran. For the calculation of autocorrelation of velocities and energy spectra, subroutines from the Numerical Recipes for Fortran [13] were implemented in the programs using Fast Fourier Transforms, FFT. The calculations were conducted on an IBM RISC 6000

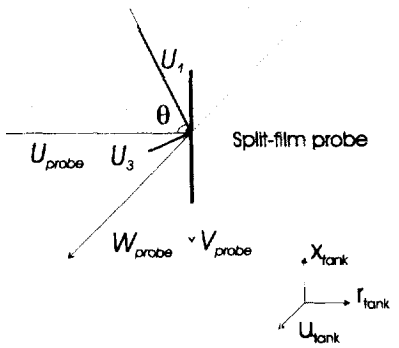

Fig. 2. Coordinate system for the split-film probe measuring in the radial/tangential (r_{tank}, Φ_{tank}) plane of the tank. U_1 is the convective flow with the direction x_1.

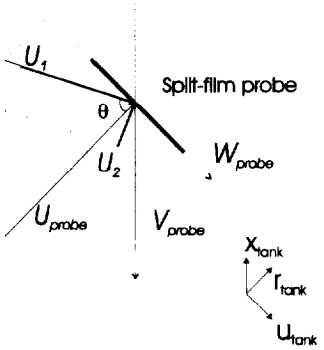

Fig. 3. Coordinate system for the split-film probe measuring in the radial/axial plane (r_{tank}, x_{tank}) plane of the tank. U_1 is the convective flow with the direction x_1.

computer with 80 MB internal memory. The sample time was chosen so that the total number of samples was 2^M, since one of the evaluation programs calculates Fast Fourier Transforms of the signal. 2^{22} (= 4,194,304) data were collected at a frequency of 10 or 15 kHz.

2.1. Scaling of statistical properties of velocity measurements

The local velocity measurements were analysed with statistical methods using Eqs. (1)–(4), resulting in the mean velocity, $\bar{U}_i$, the root mean square of the fluctuations, $\sqrt{\vec{u}_i^2}$, the skewness, S_i and the flatness, F_i, of the fluctuations. B is the one-dimensional probability density function.

$$\bar{U}_i = \int_{-\infty}^{\infty} U_i B(U_i)\,\mathrm{d}U_i \tag{1}$$

$$\sigma_{u_i}^2 = \vec{u}_i^2 = \int_{-\infty}^{\infty} u_i^2 B(u_i)\,\mathrm{d}u_i \tag{2}$$

$$S_i = \frac{\vec{u}_i^3}{\sigma_{u_i}^3} = \frac{\int_{-\infty}^{\infty} u_i^3 B(u_i)\,\mathrm{d}u_i}{\sigma_{u_i}^3} \tag{3}$$

$$F_i = \frac{\vec{u}_i^4}{\sigma_{U_i}^4} = \frac{\int_{-\infty}^{\infty} u_i^4 B(u_i)\,\mathrm{d}u_i}{\sigma_{u_i}^4} \tag{4}$$

The convective velocity, U_{conv}, has previously been defined as the mean velocity at the measuring site, assuming that the Taylor hypothesis is valid (Rao and Brodkey [2]; Komasawa et al. [14]; Günkel and Weber [3,15]; Nishikawa et al. [9]; van der Molen and van Maanen [16]; Laufhütte and Mersmann [10]). In highly turbulent flow, however, there is also a contribution to the convective velocity from the fluctuations, as discussed by Ståhl Wernersson and Trägårdh [12]. We performed measurements for all three velocity components, and therefore the complete equation, Eq. (5), based on Heskestad's equations [17], was used to determine the convective velocity.

$$U_{conv}^2 = \bar{U}_1^2 + \vec{u}_1^2 + 2\vec{u}_2^2 + 2\vec{u}_3^2 \tag{5}$$

The same expression was used by Wu and Patterson [4] and Okamoto et al. [18] but in the latter article isotropic flow was assumed and therefore $\vec{u}_1^2 = \vec{u}_2^2 + 2\vec{u}_3^2$.

The turbulent intensity of the flow, I_i, is expressed as the r.m.s. of the fluctuations normalized to a reference velocity, U_{ref}, as in Eq. (6).

$$I_i = \frac{\sqrt{\vec{u}_i^2}}{U_{ref}} \tag{6}$$

Throughout the literature on turbine-agitated tanks, both local intensities and global intensities are used. Local intensities refer to a velocity measured in the local flow position, which is usually assumed to be the convective velocity, U_{conv}. The global intensity refers to a flow variable assumed to be characteristic for the tank, for example, the impeller tip speed, V_{tip}.

2.2. Scaling of spectral properties

The turbulence of the flow can be described by an energy spectrum, where the amplitude of the fluctuations is a function of the frequencies measured. The relation of the velocity fluctuations, $u_1(t)$, to $\vec{u}_1^2$ is defined by the one-dimensional energy spectrum, $E_1(f)$, according to Eq. (7).

$$\vec{u}_1^2 = \int E_1(f)\,\mathrm{d}f \tag{7}$$

The energy spectrum is converted into a wavenumber spectrum and the following equations, Eqs. (8) and (9), are used, with U_{conv} as the characteristic flow velocity.

$$k = \frac{2\pi f}{U_{conv}} \tag{8}$$

$$E(k) = \frac{U_{conv}}{2\pi} E_1(f) \tag{9}$$

The scaling parameters for wavenumber spectra are the energy dissipation lengths, both in the convective direction, λ_f, and in the directions perpendicular to the convective direction, λ_g. These are calculated from the Eulerian time scale, $\tau_{E,i}$, as expressed by Eqs. (10)–(12).

$$R_{E,i}(t) = \frac{\overline{u_i(\tau)u_i(\tau - t)}}{\vec{u}_i^2} \tag{10}$$

$$\frac{1}{\tau_{E,i}^2} = -\frac{1}{2}\left[\frac{\partial^2 R_{E,i}}{\partial t^2}\right] \tag{11}$$

$$\lambda_i = U_{conv}\tau_{E,i} \quad i = 1 \rightarrow \lambda_f \quad i = 2,3 \rightarrow \lambda_g \tag{12}$$

Kolmogorov's scales are often used as scaling parameters, especially for measurements in pipe flow (Hintze [19]). Kolmogorov's length and velocity scales are given in Eqs. (13) and (14).

$$l_K = \left(\frac{\nu^3}{\varepsilon}\right)^{1/4} \quad (13)$$

$$\nu_K = (\nu\varepsilon)^{1/4} \quad (14)$$

2.3. Scaling of turbulent parameters in the flow

The turbulent kinetic energy, q, is defined by Eq. (15).

$$q = \frac{1}{2}(\vec{u}_1^2 + \vec{u}_2^2 + \vec{u}_3^2) \quad (15)$$

The local energy dissipation rate, ε, can be calculated by integration of the energy dissipation spectrum (Nishikawa et al. [9]; Okamoto et al. [18]) or by dimensional arguments where the characteristic velocity and the characteristic length of turbulent eddies are used (Laufhütte and Mersmann [10,20]; Wu and Pattersson [4]; Kresta and Wood [21]). We have compared these methods with the method based on Kolmogorov's hypotheses and found the latter to be the most reliable in this type of high-intensity turbulent flow, (Ståhl Wernersson and Trägårdh [12]). Therefore, local energy dissipation rates were calculated from Kolmogorov's hypothesis, which states that if the inertial subrange of wavenumbers is acquired, the one-dimensional energy spectrum is proportional to the power 2/3 of the local energy dissipation rate, according to Eq. (16).

$$E(k) = A\varepsilon^{2/3}k^{-5/3} \quad \mathrm{Re}_\lambda^{3/4} \gg 1 \quad (16)$$

The coefficient A is set to 0.47, as by Grant et al. [22]. Other values: 0.53 for pipe flow and 0.55 and 0.51 for outer layers and inner layers of shear flow, have been reported in the literature (Lawn [23]).

3. Results and discussion

3.1. Scaling of statistical properties of velocity measurements

The mean velocities were found to increase with increasing impeller speed, in the convective direction of the impeller flow, see Fig. 4a. In the perpendicular directions, x_2 and x_3, the mean velocities $\bar{U}_2$, $\bar{U}_3$ are rather close to zero is expected due to the orientation of the probe. In this figure the velocities are normalized to V_{tip}, thus indicating that V_{tip} is not a good scaling parameter for highly turbulent flow. If the same velocities are normalized to the convective velocity at the flow site, according to Eq. (5), there is only a slight increase in the mean velocities in the convective direction, as shown in Fig. 4b. In the bulk flow, the mean velocities are constant, both when scaled with V_{tip} and with the convective velocity, since the magnitude of the mean velocities is lower.

Intensities, as expressed by Eq. (6), scaled with V_{tip} and convective velocity are shown in Fig. 5a and b, respectively. In the impeller flow, there is an obvious increase in the fluctuations in the convective direction as the agitation rate is increased. When the fluctuations in the impeller flow are scaled with the convective velocity, there is, as expected, a less pronounced increase as a function of the agitation rate. Intensities in the other directions are either constant or show a slight decrease as the agitation rate is elevated.

Upon comparing local and global scaling of mean velocity and fluctuation velocity, it is obvious that local scaling better describes the flow structure, while scaling by global values gives values related to a specific reactor. In contrast to previous investigations, the graphs indicate a dependence on impeller speed.

In Fig. 6a and b the higher moments, skewness and flatness are shown, both for the impeller flow and the bulk flow. Neither the bulk flow nor the impeller flow reveals skewness or flatness factors close to a normal distribution, $S_i = 0$ and $F_i = 3$. Non-randomness of the flow is indicated by the skewness factor, which is not particularly influenced by the agitation rate, either in the impeller flow or the bulk flow. Thus, as expected, this flow is characterized by turbulent structures typical for shear flows.

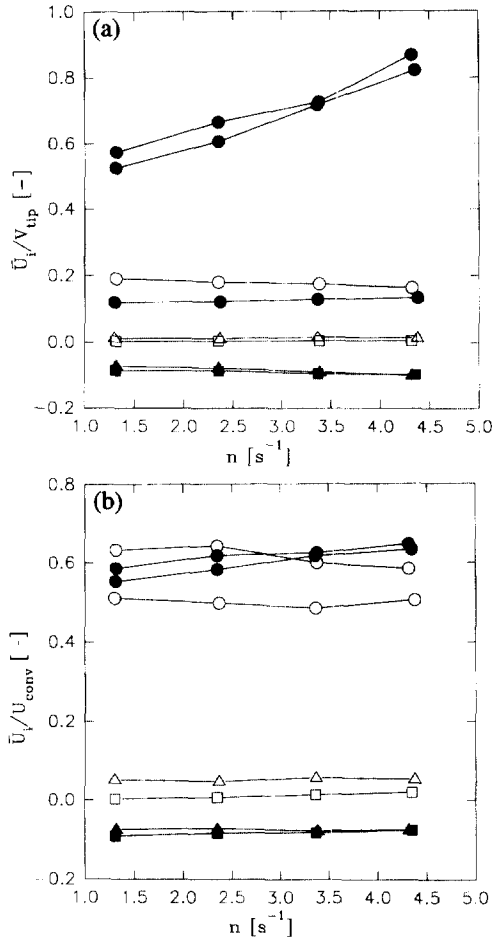

Fig. 4. (a) Mean velocities, $\bar{U}_i$ normalized to V_{tip} for three directions of flow in the impeller zone, ●x_1, ■x_2, ▲x_3 and in the bulk zone, ○x_1, □x_2, △x_3. (b) Mean velocities, $\bar{U}_i$ normalized to the convective velocity, U_{conv} for three directions of flow in the impeller zone, ●x_1, ■x_2, ▲x_3 and in the bulk zone, ○x_1, □x_2, △x_3.

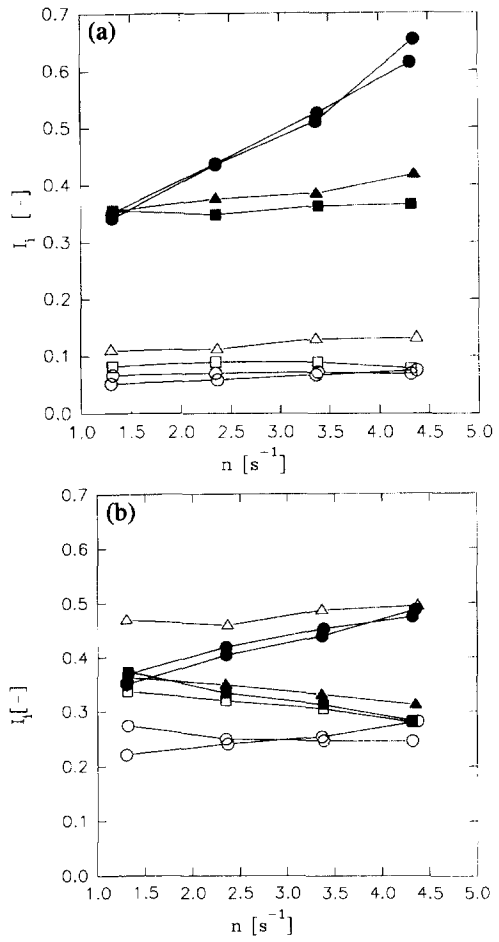

Fig. 5. (a) Turbulent intensities using V_{tip} as the reference velocity, for three directions of flow in the impeller zone, ●x_1, ■x_2, ▲x_3 and in the bulk zone, ○x_1, □x_2, △x_3. (b) Turbulent intensities using the convective velocity, U_{conv} as the reference velocity, for three directions of flow in the impeller zone, ●x_1, ■x_2, ▲x_3 and in the bulk zone, ○x_1, □x_2, △x_3.

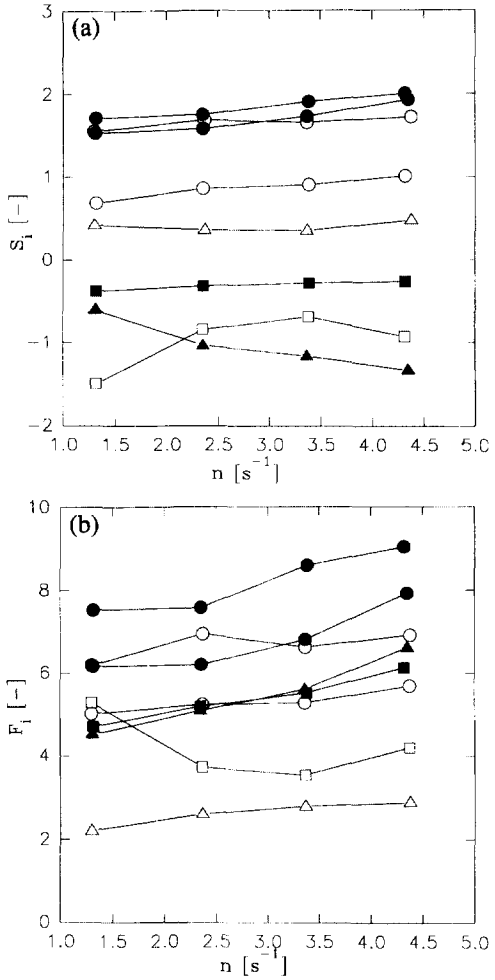

Fig. 6. (a) Skewness, S_i for three directions of flow, in the impeller zone, ●x_1, ■x_2, ▲x_3 and in the bulk zone, ○x_1, □x_2, △x_3. (b) Flatness F_i for three directions of flow in the impeller zone, ●x_1, ■x_2, ▲x_3 and in the bulk zone, ○x_1, □x_2, △x_3.

3.2. Scaling of spectral properties of the flow

Wavenumber spectra from the impeller zone were scaled with the dissipation length in the perpendicular direction, Fig. 7a. The spectra for the agitation rates 2.33 Hz to 4.33 Hz overlap both in the low-wavenumber range and in the high-wavenumber range. For the lowest agitation rate, in the 1.33 Hz spectrum, however, there is a slight deviation from this overlapping which may be due to non fully developed turbulence. In Fig. 7b the dissipation length in the convective direction was used to scale the spectrum and the pattern is similar to that in Fig. 7a. Traditionally, in turbulence theory it is λ_g which is used as reference (Hinze [19]). If Kolmogorov's scales are used for scaling, as in Fig. 7c, the overlapping of the spectra only occurs in a small range of wavenumbers, where the slope of the spectrum is proportional to $k^{-5/3}$. Thus Kolmogorov's scales are only valid in a specific region of the spectrum where the flow is isotropic.

In Fig. 8a, the spectra in the convective direction in the bulk flow are normalized by λ_g. In contrast to the impeller zone, the spectra overlap for a shorter range. The spectra show a similar pattern when they are normalized by λ_f, see Fig. 8b. Normalization using Kolmogorov's scales results in a shift of the spectra with respect to their energy content. This is similar to the situation in the impeller zone. Contrary to the impeller zone, however, the Kolmogorov scales seem to scale the entire region of high wavenumbers.

The most appropriate scaling parameters, according to our findings, are the dissipation lengths, λ_g and λ_f, for the impeller flow and the bulk flow. This is in general agreement with the results of Nishikawa et al. [9]. However, in contrast to the normalized spectra of Nishikawa et al. [9] and Costes and Couderc [7,8] it can be seen in Fig. 7a and b that for $k\lambda_g < 1$ and $k\lambda_f < 1$, the spectra are almost independent of wavelength, and for $k\lambda_g > 1$ and $k\lambda_f > 1$ the spectra are clearly dependent on wavelength. Costes and Couderc [7] state that normalizing their frequency spectra with the velocity nd_{imp} as $E_1(f)/(\bar{u}_1^2/n)$ and the frequency with agitation rate, as f/n, leads to a similar appearance of the curves. However, in our measurements, this choice resulted only a parallel movement of each spectrum from low-energy spectra to high-energy spectra. Komasawa et al. [14] used macroscale as a

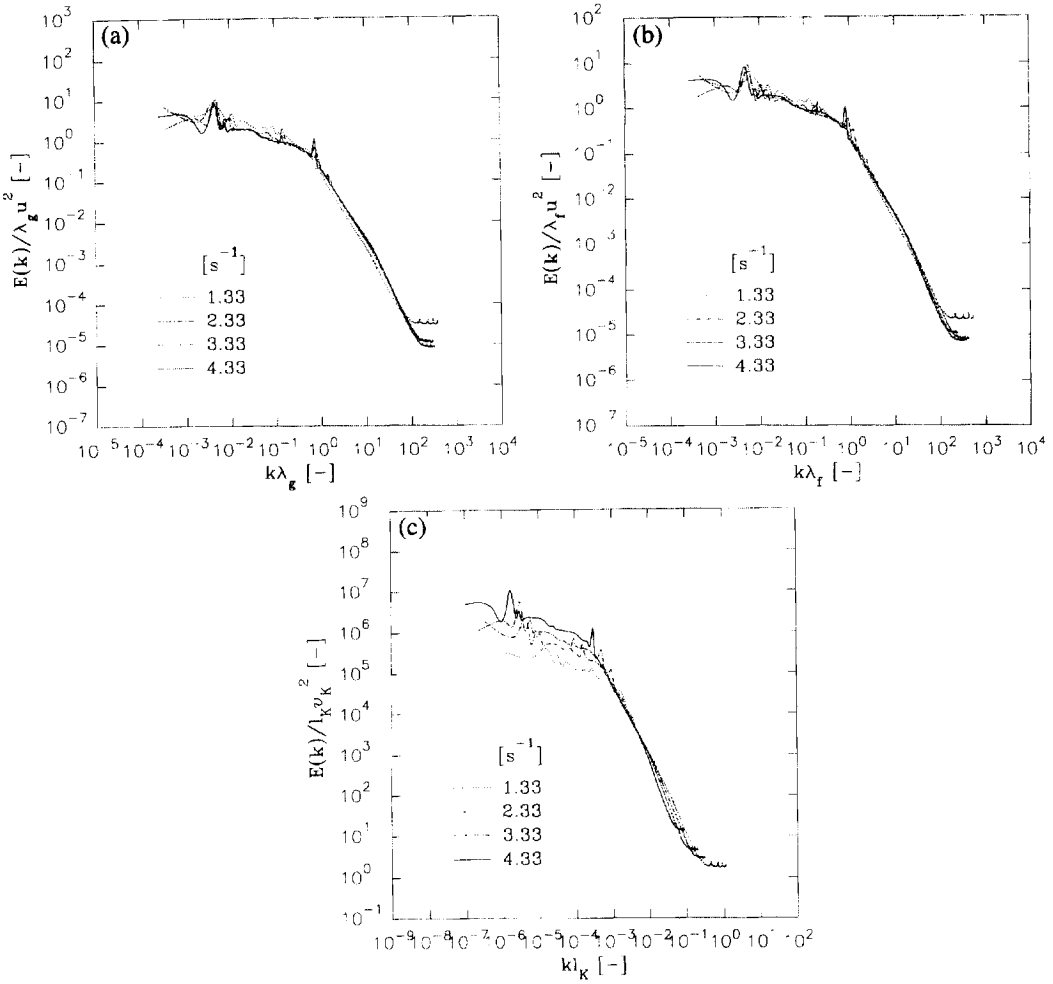

Fig. 7. (a) Energy spectra for four agitation rates in the impeller zone, scaled by the perpendicular dissipation length λ_g. (b) Energy spectra for four agitation rates in the impeller zone, scaled by the convective dissipation length λ_f. (c) Energy spectra for four agitation rates in the impeller zone, scaled by Kolmogorov's length scale l_K.

scaling parameter, where the macroscale is defined by the intercept of the energy spectrum with the y-axis using Eq. (17).

$$K=\frac{E_1(f)}{4\bar{u}_1^2} \tag{17}$$

The pattern was found to be similar to the scaling proposed by Coustes and Couderc [7], although the spread between the spectra was greater. In Table 1, the dissipation scales and the Kolmogorov scales are given for the measurements made.

3.3. Scaling of turbulent parameters in the flow

As shown in Fig. 9, the turbulent kinetic energy increases drastically with increasing agitation rate. The main reason for this is the increase in the fluctuations in the convective direction for the impeller zone (see Fig. 7a). The flow from the impeller becomes more jet like for high Reynolds numbers. There is a similar pattern in the bulk zone, but the level of turbulent kinetic energy is 10–20 times lower than in the impeller flow at a similar agitation rate.

Kolmogorov's hypothesis appears to be valid for the measurements of impeller flow, as the local energy dissipation rate determined by Eq. (16) shows no major differences depending on the direction of flow (see Fig. 10). However, in the bulk zone the local energy dissipation rate is higher in the perpendicular directions, u_2 and u_3. This may be due to the lack of a distinct convective flow direction and an aliasing error may appear in the measurements. Also, the local Reynolds numbers are low ($<10^3$).

The slopes of the log–log plots of the turbulent parameters q and ε as a function of agitation rate, n, are given in Table 2. The slopes show higher values in the impeller zone than in the bulk zone. This express the stronger production of turbulence in the impeller region than in the bulk region. It can also be seen that the local energy dissipation rate has a stronger dependency on agitation rate than the turbulent kinetic energy. This is explained by the fact that ε is proportional to $Aq^{3/2}/l$ when $q^{1/2}$ is chosen as the characteristic

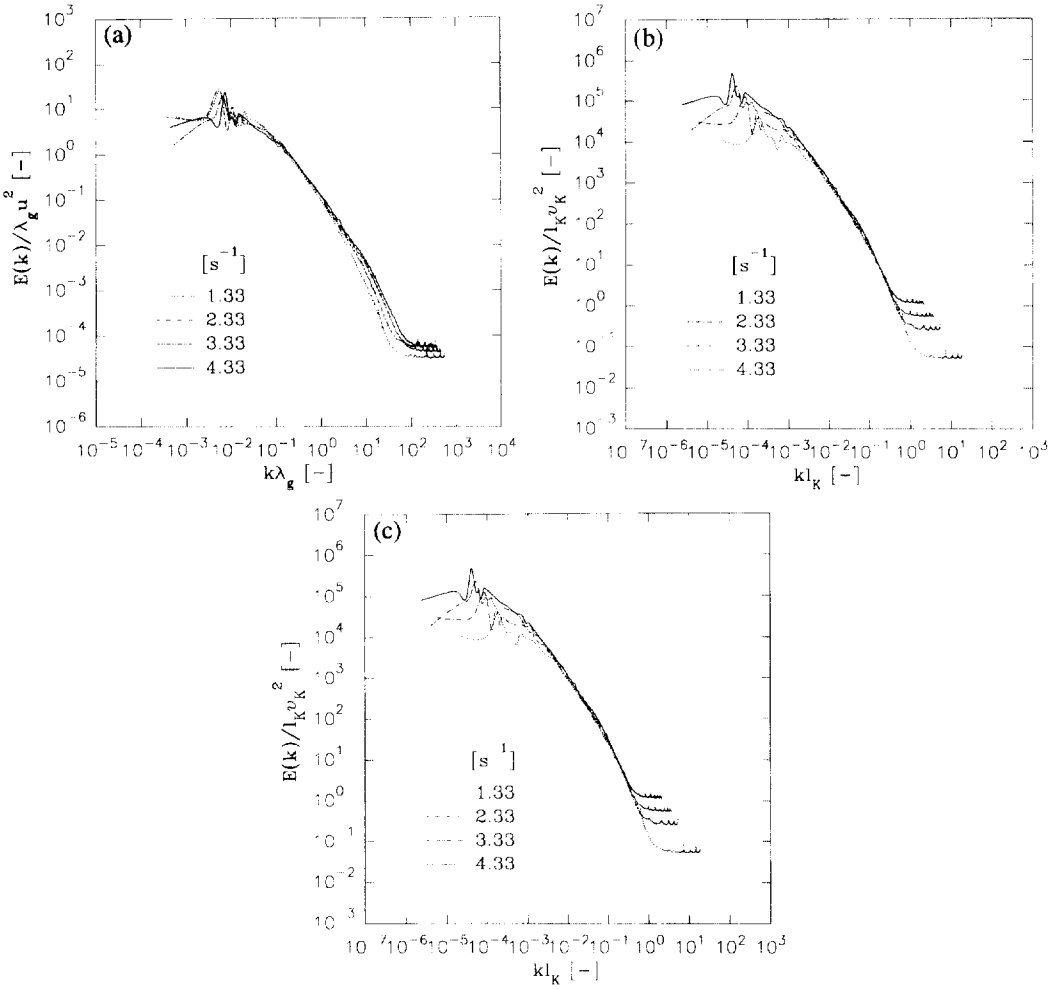

Fig. 8. (a) Energy spectra for four agitation rates in the bulk zone, scaled by the perpendicular dissipation length λ_g. (b) Energy spectra for four agitation rates in the bulk zone, scaled by the convective dissipation length λ_f. (c) Energy spectra for four agitation rates in the bulk zone, scaled by Kolmogorov's length scale l_K.

velocity and l is the characteristic length. Therefore the slope for local energy dissipation rate, ε, is 1.5 times the slope for the turbulent kinetic energy, q (see Table 2). This relation supports the use of Kolmogorov's spectrum law, Eq. (16), in the evaluation of local energy dissipation rates.

4. Conclusions

Parameters of turbulence for a turbine-agitated tank have been measured both in the impeller flow and in the bulk flow over a wide range of agitation rates. These conditions represent both actual process conditions in industrial fermentation in regard of power input per unit mass and lower energy inputs previously discussed in the literature (bench scale).

The local scaling parameter, U_{conv}, scales the mean flow and the intensity of the flow such that they are constant, both in the impeller flow and in the bulk flow. When the global scaling parameter, v_{tip}, is used, the mean velocity in the convective direction increases with tip speed in the impeller flow. A similar pattern is observed when the intensity is scaled with v_{tip}. The intensity in the convective direction increases with increasing impeller speed. The agitation rate, as used in the expression of v_{tip}, cannot be used as a scaling parameter when scaling from low-energy input to several times higher energy input.

Energy spectra, as a function of wavenumber, scale in the impeller flow with the energy dissipation lengths, λ_g and λ_f, both for the high-energy part of low wavenumbers and in the low-energy part of high wavenumbers. Kolmogorov's scales scale the spectra only for a small range of wavenumbers which are proportional to $k^{-5/3}$, where isotropic flow is achieved. In the bulk zone the energy dissipation lengths, λ_g, scale the lower wavenumber region of the spectra whereas the higher wavenumbers scale with Kolmogorov's scales. This may be due to the fact that we measured close to Kolmogorov's length scales in these positions (see Fig. 8c, $kl_K = 1$ at the limit of the measurements).

Turbulent kinetic energy and local energy dissipation rate both show a linear increase in the ratios of impeller flow measurements to bulk flow measurements, as the agitation rate is increased. This indicates that changing the operating conditions affects flow conditions in the impeller zone more than in the bulk zone. The span of turbulent kinetic energy

Table 1
Turbulent characteristics in impeller flow and bulk flow

Dissipation length					Kolmogorov's scales						Turbulent kinetic energy		Energy dissipation rate	
n [s^{-1}]	λ_f [m] · 10^3		λ_g [m] · 10^3		Re_λ [−]		v_K [m s^{-1}]		l_K [m] · 10^5		q [m^2 s^2]	q [m^2 s^2]	ε [m^2 s^{-3}]	ε [m^2 s^{-3}]
	Imp.	Bulk	Imp.	Bulk	Imp.	Bulk	Imp.	Bulk	Imp.	Bulk	Imp.	Bulk	Imp.	Bulk
1.33	18.0	4.6	12.5	4.4	870	40	0.022	0.008	3.85	14.5	0.22	0.01	0.62	0.003
2.33	27.3	5.3	20.1	5.2	1980	120	0.053	0.014	2.09	8.1	0.88	0.04	7.10	0.032
3.33	26.1	5.3	22.4	7.3	7000	320	0.079	0.019	1.40	5.9	2.16	0.12	35.4	0.12
4.33	24.3	8.3	22.6	7.7	11 600	540	0.114	0.026	0.98	4.3	4.88	0.20	150	0.39

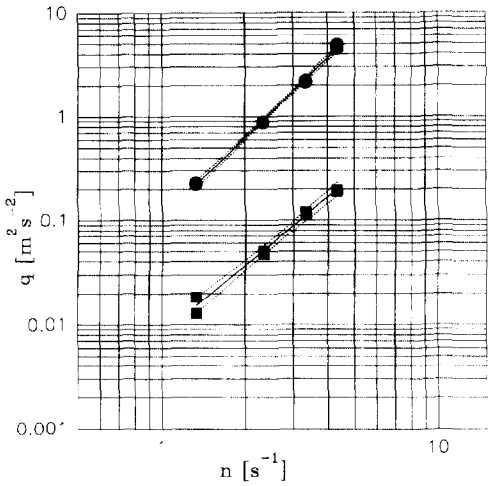

Fig. 9. Turbulent kinetic energy, q, as a function of agitation rate in the impeller zone (●) and in the bulk zone (■). The full line is linear regression of eight values. The dotted line is the standard deviation (95%).

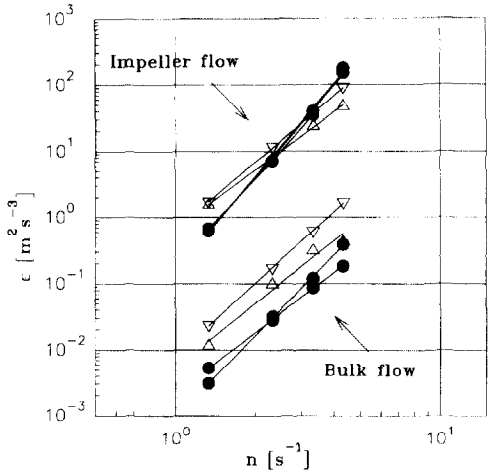

Fig. 10. Local energy dissipation rates calculated according to Kolmogorov's hypothesis, Eq. (16), in the impeller flow and the bulk flow (●x_1, ▽x_2, ▽x_3). Kolmogorov's hypothesis is valid for the impeller flow while there is aliasing in the bulk flow.

and local energy dissipation rate for these agitation rates also gives an indication of the large variations in flow conditions existing locally in a turbine-agitated tank. To our knowledge, no results have previously been presented on local energy dissipation rates in turbine-agitated tanks for this energy input range, which is comparable to that used in industrial processes.

Table 2
Regression lines in Figs. 9 and 10

Flow characteristics		Zone	Slope mean ± SD
log (Y)	log (X)		
q	n	Impeller	2.55 ± 0.04
q	n	Bulk	2.17 ± 0.09
ε	n	Impeller	3.88 ± 0.23
ε	n	Bulk	3.45 ± 0.05

5. Notation

A	[−]	coefficient
B	[−]	probability density function, PDP
ΔC	[m]	impeller spacing
d_{imp}	[m]	impeller diameter
D_{tank}	[m]	tank diameter
$E_1(f)$	[m^2 s^{-1}]	one-dimensional frequency spectrum function
$E(k)$	[m^3 s^{-2}]	one-dimensional wavenumber spectrum
f	[s^{-1}]	frequency
F_i	[−]	flatness
H_L	[−]	liquid height compared with tank diameter
$H_{v,i}$	[−]	height of measurement positions (i = 1,2)
I_i	[−]	turbulent intensity
K	[s]	macro scale
k	[m^{-1}]	wavenumber
l_K	[m]	Kolmogorov's length scale
n	[s^{-1}]	agitation rate
q	[m^2 s^{-2}]	turbulent kinetic energy
$R_{E,i}$	[−]	autocorrelation function
Re_λ	[−]	Reynolds number for energy dissipation length
r_{tank}, x_{tank}, Φ_{tank}	[−]	radial, axial, tangential tank coordinates
S_i	[−]	skewness
x_1, x_2, x_3	[−]	flow coordinates, x_1 is the convective direction

$\bar{U}$	[m s^{-1}]	ensemble time average of mean velocity $i = 1,2,3$
U_{conv}	[m s^{-1}]	convective velocity
x_{probe}, y_{probe}, z_{probe}	[−]	radial, axial and tangential probe coordinates
U_{ref}	[m s^{-1}]	reference velocity
u_i	[m s^{-1}]	velocity fluctuations, $i = 1,2,3$
$\bar{u}_i^2$	[m^2 s^{-2}]	ensemble average of velocity fluctuations, $i = 1,2,3$
$\sqrt{\bar{u}_i^2}$	[m s^{-1}]	r.m.s of the velocity fluctuations, $i = 1,2,3$
V_{tip}	[m s^{-1}]	tip velocity
Greek letters		
ε	[m^2 s^{-3}]	energy dissipation rate
λ_f, λ_g	[m]	energy dissipation length scales, Taylor's microscale
τ_E	[s]	Eulerian time scale
θ	[°]	angle for calibration
υ	[m^2 s^{-1}]	kinematic viscosity
$\sigma_{u_i}^2$	[−]	variance
υ_K	[m s^{-1}]	Kolmogorov's velocity scale

Acknowledgements

This work is part of the project Bioreactor Performance within the Nordic Bioprocess Engineering Programme and the Bioprocess Technology programme. Both programmes are funded by the Swedish National Board for Industrial and Technical Development, NUTEK. Their support is gratefully acknowledged. We would also like to thank Scaba, Sweden, who kindly supplied the agitation system and the Rushton turbines.

References

[1] A.S. Mujumdar, B. Huang, D. Wolf, M.E. Weber, W.J.M. Douglas, Can. J. Chem. Eng. 48 (1979) 475–483.
[2] M.A. Rao, R.S. Brodkey, Chem. Eng. Sci. 27 (1972) 137–156.
[3] A.A. Günkel, M.E. Weber, AIChE J. 21 (1975) 931–939.
[4] H. Wu, G.K. Patterson, Chem. Eng. Sci. 44 (1989) 2207–2221.
[5] S.M. Kresta, P.E. Wood, AIChE J. 37 (1991) 448–460.
[6] L. Cutter, AIChE J. 12 (1996) 35–45.
[7] J. Costes, J.P. Couderc, Chem. Eng. Sci. 43 (1988) 2751–2764.
[8] J. Costes, J.P. Couderc, Chem. Eng. Sci. 43 (1988) 2764–2772.
[9] M. Okamoto, Y. Nishikawa, K. Hashimato, S. Nagata, Turbulence energy spectra in baffled mixing vessels, Chem. Eng. Japan, 1976, pp. 489–494.
[10] H.D. Laufhütte, A. Mersmann, Dissipation of power in stirred vessels, Paper No. 33, 5th European Conf. on Mixing, Würtzberg, 1985, pp. 331–340.
[11] Y. Kawase, M. Moo-Young, Chem. Eng. J. 43 (1990) B19–41.
[12] E. Ståhl Wernersson, Ch. Trägårdh, Measuring and analysis of high intensity turbulent characteristics in a turbine agitated tank, manuscript in preparation.
[13] W.H. Press, S.A. Teukolsky, W.T. Vetterling, B.P. Flannery, Numerical Recipes in Fortran, 2nd edn., Cambridge, 1992.
[14] I. Komasawa, R. Kuboi, T. Otake, Chem. Eng. Sci. 29 (1974) 641–650.
[15] A.A. Günkel, M.E. Weber, AIChE J. 21 (1975) 939–948.
[16] K. Van der Molen, H.R.E. Van Maanen, Chem. Eng. Sci. 33 (1978) 1161–1168.
[17] G. Heskestad, J. Appl. Mech. 32 (1965) 735–739.
[18] Y. Okamato, M. Nishikawa, K. Hashimoto, Int. Chem. Eng. 21 (1981) 88–94.
[19] J. Hinze, Turbulence, 2nd edn., 1975.
[20] H.D. Laufhütte, A. Mersmann, Chem. Eng. Technol. 10 (1987) 56–63.
[21] S.M. Kresta, P.E. Wood, Chem. Eng. Sci. 48 (1993) 1761–1774.
[22] H.L.R. Grant, W. Stewart, A. Moilliet, J. Fluid Mech. 12 (1962) 241–263.
[23] C.J. Lawn, J. Fluid Mech. 48 (1971) 477–505.